

Heat Transfer Performance Evaluation of Common Flow-Down Rectangular Winglet Vortex Generator in Solar PV Cooling System

Syahru Ramadhan Putra

Department of Mechanical Engineering, Faculty of Engineering, Universitas Sebelas Maret, Surakarta 57126, Indonesia

Dominicus Danardono Dwi Prija Tjahjana

Department of Mechanical Engineering, Faculty of Engineering, Universitas Sebelas Maret, Surakarta 57126, Indonesia

Indri Yaningsih

Department of Mechanical Engineering, Faculty of Engineering, Universitas Sebelas Maret, Surakarta 57126, Indonesia

<https://doi.org/10.5109/7411070>

出版情報 : Evergreen. 13 (1), pp.294-306, 2026-03. 九州大学グリーンテクノロジー研究教育センターバージョン :

権利関係 : Creative Commons Attribution 4.0 International



Heat Transfer Performance Evaluation of Common Flow-Down Rectangular Winglet Vortex Generator in Solar PV Cooling System

Syahru Ramadhan Putra¹, Dominicus Danardono Dwi PrijaTjahjana¹,
Indri Yaningsih^{1,*}

¹Department of Mechanical Engineering, Faculty of Engineering, Universitas Sebelas Maret, Surakarta 57126, Indonesia

*Author to whom correspondence should be addressed:

E-mail: indriyaningsih@staff.uns.ac.id

(Received May 24, 2025; Revised January 29, 2026; Accepted March 09, 2026)

Abstract: The increase in temperature on the surface area of solar photovoltaic (PV) panels can lead to a reduced lifespan. One potential solution for reducing their temperature is the implementation of a cooling system. This study investigates the effect of a Rectangular Winglet Vortex Generator (RWVG) arranged in a Common Flow Down (CFD) configuration on heat transfer in solar PV cooling. The RWVG is made of aluminium. The experimental study was conducted at various angles of attack (AoA) of 30°, 50°, 60°, and 70°, across a Reynolds number range of 15,000 to 45,000. The results showed that the RWVG significantly increased both the heat transfer coefficient and the Nusselt Number (Nu). Notably, at an AoA of 60°, there was a 92.45% improvement in heat transfer, which corresponded to a 25% reduction in temperature. Furthermore, the paired configuration of the RWVG proved to be more effective than the single configuration, indicating that the RWVG can enhance the cooling efficiency of solar PV systems and optimize their thermal performance. These findings were further supported by visualizations from an infrared thermal camera, which showed the areas cooled by the presence of the vortex generator.

Keywords: Common Flow Down; Solar PV Cooling; Thermal Performance; Vortex Generator

1. Introduction

The depletion of fossil fuels, coupled with global warming, has led to an increased interest in the use and development of renewable energy sources¹. Among these, solar energy stands out as a promising method for generating electricity in residential, commercial, and industrial settings. One common application of solar energy is through photovoltaic (PV) solar panels. These panels contain PV cells that convert solar radiation into electrical energy². However, many PV solar panels have low efficiency when it comes to converting solar radiation into electricity^{3,4}. Typically, only about 15% of the total solar radiation is transformed into electrical energy, while the remaining 85% is converted into heat energy^{5,6}. This excess heat can raise the temperature of the PV solar panels, and if temperatures exceed certain limits, it can negatively impact the panels' electrical efficiency and lead to corrosion, ultimately shortening their lifespan⁷. To ensure that photovoltaic (PV) solar panels operate at optimal temperatures, it is crucial to develop an effective cooling

system. The ideal operating temperature for commercial solar PV panels usually ranges from 15°C to 35°C⁸. However, during peak sunlight hours, the surface temperature of the panels can reach as high as 70°C⁹. The surface temperature is influenced by several factors, including ambient temperature, wind speed, and solar irradiation.

Various methods have been implemented to regulate the surface temperature of PV systems, utilizing effective thermal engineering practices. This regulation ensures that temperatures do not exceed safe limits and remain close to the standard test condition of 25°C, which is optimal for maximizing efficiency^{10,11}. Several cooling strategies have been shown to effectively reduce thermal loads and extend the lifespan of PV systems¹². Typically, temperature reduction is achieved through passive cooling methods, which do not require electrical power or mechanical devices¹³. One widely used passive cooling technique to enhance thermal performance is the use of Vortex Generators (VGs).

A vortex generator (VG) is a small fin-shaped component

typically found on the wings or tail stabilizer surfaces of vehicles, designed to modify airflow. Vortex generators can be surfaces that protrude or stick out from the main surface. They create vortices through the friction and separation of the airflow that interacts with them¹⁴). In addition to their simplicity and efficiency, adding VGs to PV solar panels helps the panels absorb more heat by disrupting the airflow entering the panels¹⁵).

There are four basic types of VGs: delta wing, rectangular wing, delta winglet, and rectangular winglet¹⁶). Delta wing VGs produce transverse vortices, while winglet types generate longitudinal vortices. Winglet-type VGs create high-quality vortices that can persist further downstream from the surface¹⁷). Flow configurations can be categorized as either common flow up (CFU) or common flow down (CFD). In a CFD configuration, the transverse distance between the leading edges of the longitudinal vortex pair is smaller than the distance between their trailing edges and vice versa in a CFU configuration. The configuration and positioning of the VGs significantly affect the speed and direction of the incoming airflow¹⁸).

Several studies have been conducted on VG to improve heat transfer. One such study by Suryo et al.¹⁹) examined the impact of the aspect ratio of delta winglet vortices on heat transfer within a channel. They investigated how heat transmission holes and flow structures varied with Reynolds numbers (Re) ranging from 400 to 2,000. By using these configurations and variations, the results of the study showed that the holes in the VG had a small effect on reducing the convection heat transfer coefficient, and the effect of the jet flow holes weakened the longitudinal vortex (LV), so that it had an effect on increasing heat transfer. Silva et al.²⁰) conducted a study using two types of VGs rectangular and delta winglets placed inside a circular tube of a solar collector. Their results indicated that the optimal ratio between heat transfer and pressure drop penalty was achieved with the delta wing at an angle of attack of 30°. Additionally, the rectangular winglet VG produced the highest heat transfer results at an angle of attack (AoA) of 45°. Lei et al.²¹) and Wang et al.²²) stated that the optimal ratio of length to height for delta-type VGs is 2. Furthermore, Mohanakrishnan et al.²³) noted that heat transfer enhancement occurs when the transverse distance between VGs is twice the height of the wings.

Dezan et al.²⁴) continued their research on solar air heating channels by adding a pair of non-periodic rectangular wings to the absorber plate. In the study, the rectangular wings in the first row have an important role in increasing heat transfer and pressure penalty. In the CFU configuration, these wings create a more robust vorticity structure compared to the CFD configuration. However, optimizing the CFD configuration yields better performance than the CFU configuration when operating at a Re of 10,000²⁴).

Modi et al.²⁵) continued their research on fin-tube heat

exchangers (FTHE) that utilize rectangular winglet-type VGs. In their study, they discovered that a lower tube surface temperature results in the greatest enhancement of heat transfer performance while also maintaining a lower friction factor. Additionally, they found that the thermal performance factors for rectangular winglets with circular holes were higher than those of rectangular flat wings, with increases of 1.04-3.2%, 1.3-5.4%, and 2.3-10.52% for tube temperatures of 65°C, 75°C, and 85°C, respectively.

Research on the addition of VGs was conducted by Heriyani et al.²⁶). The study focused on a fin tube heat exchanger that utilized a concave rectangular winglet-type VG mounted on a plate within a rectangular channel. This design aimed to enhance heat transfer through six heating tubes into the air flow. The findings revealed an increase in thermal performance by a factor of 1.29, with staggered configurations yielding better critical blockage ratios (CBR) compared to in-line arrangements²⁶). Additionally, Sarangi and Mishra²⁷) conducted a comprehensive study on the heat addition technique supported by VGs in heat exchange applications. Their research demonstrated that the longitudinal flow created by the VG can reduce the wake area behind the tube, thereby enhancing flow mixing and increasing turbulence strength.

Sheikholeslami and Abd Ali²⁸) conducted an experimental study on enhancing concentrated photovoltaic thermal systems using VGs. They found that the presence of VGs maximized heat dissipation, and when they modified the flow rate, the VGs not only improved cooling efficiency but also reduced pumping power by up to 50%, particularly when a concentrator was used. The use of VGs for cooling solar cells significantly increased power production. Additionally, Souayeh et al.²⁹) investigated heat transfer enhancement in solar PV systems by modifying the surface area with wavy channels. These wavy channels expanded the surface area while creating secondary flow patterns. Choi et al.³⁰) improved the heat transfer performance of solar PV cooling by using channels imprinted with dimple arrays under various flow conditions. The inclusion of the dimple array in the cooling channel had a substantial impact on heat transfer performance, achieving a thermal performance factor 1.8 times greater than that of channels without dimples. Furthermore, Ali et al.³¹) optimized the design of the winglet vortex generator by exploring the best combination of attack and inclination angles. The presence of VGs with an optimal AoA significantly enhanced heat transfer performance by mixing the flow field, which was induced by local vortices.

Several studies indicate that proper cooling of solar photovoltaic (PV) panels can enhance their performance. The use of Vortex Generators (VGs) is still relatively uncommon in existing research; however, VGs have shown potential for effective cooling of solar PV systems^{32,33}). Zhou et al.³³) investigated the attachment of vortex generators (VGs) to the rear surface of photovoltaic

(PV) modules. They found that under free convection conditions, the presence of VGs reduced PV temperatures by 2-3°C. In a subsequent outdoor experiment, Zhou et al.³⁴⁾ studied the effects of delta winglet VGs on the rear surface of solar PV modules. Their results showed that the roof-mounted vortex generator (RWVG) configuration could reduce temperatures by 1.5°C under low-wind conditions and by 2.5°C under high-wind conditions. The VGs were made of aluminum, and two factors contributed to the temperature reduction: the dominant convection driven by the low wind speed and the material's heat-conduction properties as a heat sink. In 2025, Sheikholeslami and Ali³⁵⁾ evaluated the use of VGs for enhancing the performance of solar PV system. They employed two methods: an active method that utilized circulated coolant water and a passive method that used VGs. Under low wind conditions, the combination of VGs and the water coolant resulted in a temperature reduction of up to 2.5°C in the PV modules. Additionally, Marausna et al.³⁶⁾ conducted a study on a hybrid method that combined wavy VGs with a water cooling channel. They discovered that this hybrid cooling system significantly improved heat removal. Furthermore, their research indicated that the geometry of the VGs affects how effectively the water coolant transports heat away.

Based on the literature reviewed, we found that vortex generators (VGs) show promise in reducing the temperature of solar photovoltaic (PV) panels, with their geometry significantly influencing heat transfer. The referenced studies indicate that VGs are primarily placed on the rear side of the PV panel. In this manuscript, we propose a novel PV cooling system where the design of the VGs, both their shape and dimensions, is tailored according to the selected Reynolds number. Moreover, the VGs have been strategically positioned on the front surface of the PV panels to effectively disrupt airflow while ensuring that light penetration remains unobstructed and vortices are not weakened. The photovoltaic (PV) panels have been configured horizontally to enhance airflow across their surfaces. This study aims to develop a passive cooling solution for solar PV panels utilizing vortex

generators (VGs). The focus will be on investigating the effects of incorporating rectangular winglet-type VGs (RWVGs) within a common flow-down (CFD) configuration. The main objective of this research is to evaluate potential improvements in heat transfer specifically in terms of the heat transfer coefficient and the Nusselt Number (Nu) on solar PV panels using vortex generators (VGs). Additionally, thermal visualization techniques will be employed to validate the phenomena observed throughout the study.

2. Experimental Design

2.1. Experimental Components

The experimental scheme in this study is illustrated in Figure 1, which consists of a subsonic wind tunnel, a PV solar panel model, a thermal camera, a thermocouple, and a vortex generator.

This experimental setup features a subsonic wind tunnel, with a designated test section in the middle. Within this test section, an aluminum plate is equipped with a heater to simulate a solar photovoltaic (PV) model. A Type C thermocouple is attached to the plate, positioned centrally at the back, to measure temperature during testing. Additionally, a transparent window is installed at the bottom of the test section to facilitate visual data collection using a thermal camera, allowing for easier photography of the solar PV model. At the rear of the setup, a blower is utilized to circulate air through the test section. This blower has a power rating of 4 kW and can achieve air speeds of up to 30 m/s.

Figure 2(a) displays the Single Configuration, where the distance between the RWVGs is $W = 29.95$ mm. Meanwhile, Figure 2(b) presents a common flow-down paired configuration, which consists of two pairs of RWVGs. Each pair has a front edge distance of $b = 14.775$ mm, and the distance between the pairs of RWVGs is also $W = 29.95$ mm. In both configurations, a total of four RWVGs are installed at the inlet of the solar PV model, which features a flat base that aligns with the surface of the model.

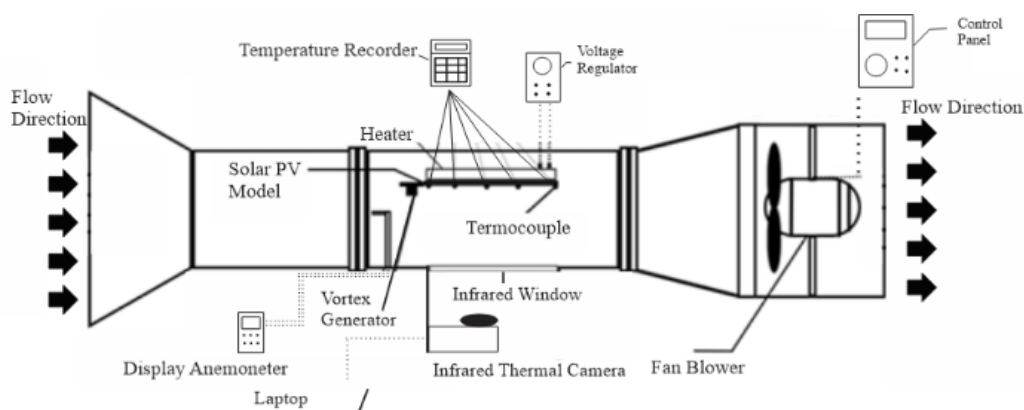


Fig. 1: Experimental Setup

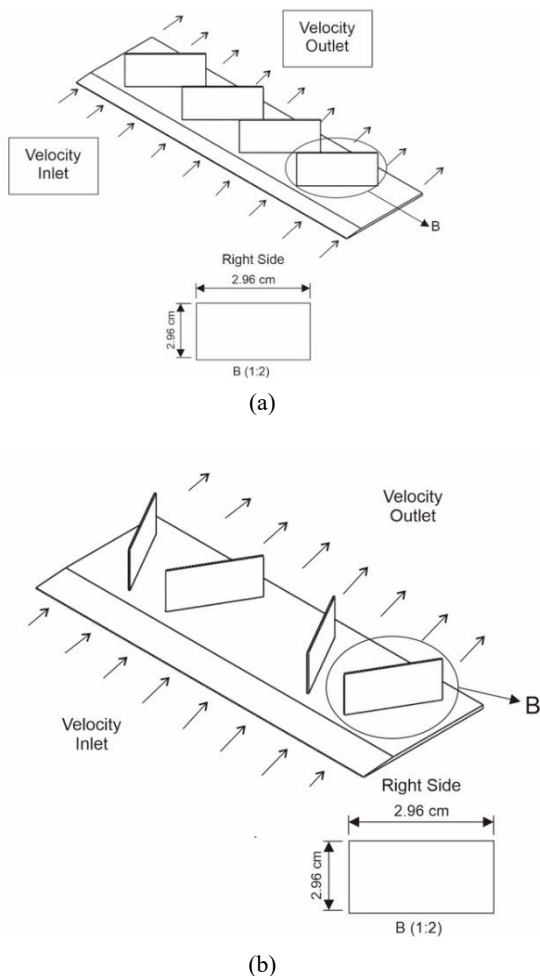


Fig. 2: RWVG (a) Single and (b) Pair (common flow down) configuration

The rectangular winglet vortex generator (RWVG) is constructed from an aluminum plate, as this material is readily available, easy to cut, and simple to shape. The manufacturing process of the RWVG is carried out manually and involves cutting and bending stages. The dimensions of the RWVG are as follows: a height of $H = 14.775$ mm, a length of $L = 29.95$ mm, and a thickness of $b = 0.1$ mm, as illustrated in Figure 2.

In this study, a solar PV model made of aluminum alloy A1100 with a thickness of 3 mm was selected due to its rust-resistant properties and availability. The dimensions of the solar PV model are 305 mm x 195 mm, which were designed to fit the hydraulic diameter of the wind tunnel, as illustrated in Figure 3.

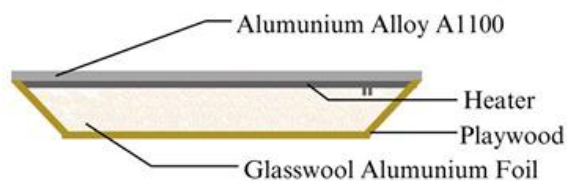


Fig. 3: Solar PV Model

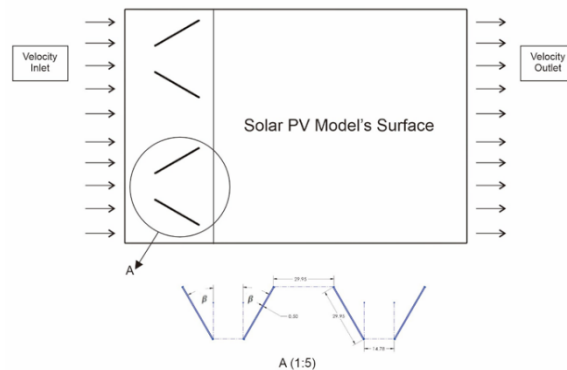


Fig. 4: Schematic diagram of the attachment of VGs in the solar PV model's surface

The heater, which is placed beneath the flat plate, provides heat to the solar PV model and has a power capacity of 1200 W. To enhance thermal insulation, Glasswool Aluminum Foil is positioned under the heater, helping to prevent heat loss due to the cooling airflow from the blower. This glass wool can effectively insulate heat up to 121°C. The heater's temperature is controlled by an OKI Voltage Regulator, model TDGC2-2000, which has a maximum output voltage of 250 VAC. This setup ensures that the heat flux received by the solar PV model remains at a constant temperature.

Five T-type thermocouples are installed in line on the surface of the solar PV model, with a distance of 75 mm between each thermocouple from the inlet to the outlet end of the channel. These thermocouples can detect temperatures ranging from 0°C to 200°C. To display the measurement results from the thermocouples, an additional device is required. Therefore, the thermocouples are connected to a data acquisition system, specifically a temperature recorder. The device used for this purpose is the Lutron BTM-4208SD, which has a data reading accuracy of $\pm 0.4\%$. The airflow velocity entering the test section was measured using a Benetech GT8907 Digital Anemometer. This device measures air velocity ranging from 0.4 m/s to 25 m/s, with an accuracy of $\pm 3.5\%$. Additionally, it can detect room temperature. In this study, the airflow velocity was varied to 0.8, 1.2, 1.6, and 2 m/s to provide effective cooling on the surface of the solar PV model. The schematic diagram of the VG placement in solar PV is shown in Figure 4. As can be observed, the VG was installed in front of the solar PV panel surface.

2.2. Convection Heat Transfer Equation and Testing

The source of heat is represented by the heat flux received by the solar PV model. This model will be heated according to the heat flux data from Surakarta City, with a constant power of 70 W. The heat flux data was obtained from the Indonesian Solar Energy Association and is applied with a constant value since the voltage (V) and electric current (I) are in stable conditions.

Heat flux (q'') in solar PV models can be calculated using the following equation:

$$q'' = \frac{V_{electric} \cdot I}{A_s} \quad (1)$$

In this context, $V_{electric}$ represents the voltage across the heater (V), I denotes the electric current passing through the heater (A), and A_s refers to the surface area of the solar PV model (m^2).

The heat transfer coefficient can be calculated using the heat flux from the solar PV model along with the surface temperature recorded by the temperature sensor. This can be determined using the following equation:

$$h = \frac{q''}{(T_s - T_\infty)} \quad (2)$$

Where h is the convection heat transfer coefficient ($W/m^2 \cdot K$), q'' represents the heat flux (W/m^2), T_s denotes the surface temperature of the solar PV model (K), and T_∞ is the ambient room temperature (K).

The Reynolds number (Re) can be calculated from the air velocity entering the test section using the following equation:

$$Re = \frac{V \cdot H}{\nu} \quad (3)$$

Where V represents the air velocity (m/s), H denotes the height of the RWVG (m), and ν stands for kinematic viscosity (m^2/s).

The effectiveness of heat transfer from the surface of the solar PV model to the air can be assessed by calculating the Nusselt number (Nu) using the following equation:

$$Nu = \frac{h \cdot H}{k} \quad (4)$$

In this context, h represents the convection heat transfer coefficient ($W/m^2 \cdot K$), H is the height of the RWVG (m), and k is the thermal conductivity ($W/m \cdot K$).

Thermal performance in convection heat transfer refers to a system's ability to conduct or retain heat. Dimensionless similarity parameters are crucial because they allow the application of results obtained from experiments to surfaces subjected to convective conditions. As such, the Nusselt number can be used to demonstrate the impact of incorporating RWVG into the solar PV model. The thermal performance in this study can be evaluated through the following comparison:

$$\text{Thermal Performance (TP)} = \frac{Nu_{vG}}{Nu} \quad (5)$$

Where Nu_{vG} is the Nusselt number resulting from the addition of RWVG, and Nu_0 is the Nusselt number without the addition of RWVG.

2.3. Infrared Thermography

An infrared thermography system was utilized to visualize temperature changes on the surface of the solar photovoltaic (PV) model. This was achieved using a FLIR C5 thermal camera connected to a laptop equipped with FLIR Thermal Studio software. The thermal camera measures temperatures ranging from $-20^\circ C$ to $400^\circ C$, with an image frequency of 8.7 Hz. It has an accuracy of $\pm 3.5\%$, a field of view of $54^\circ \times 42^\circ$, and a resolution of 160×120 pixels. The images captured by the thermal camera serve as corroborating evidence that RWVG enhances convection heat transfer on the surface of the solar PV model by illustrating its surface temperature distribution.

3. Results and Discussion

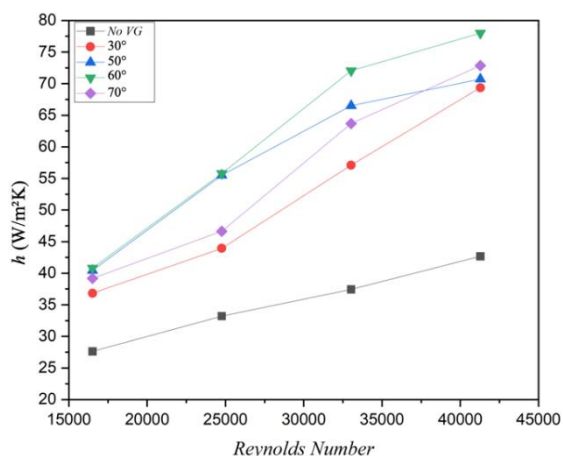
3.1. The effect of Rectangular Winglet Vortex Generator (RWVG) on Convection Heat Transfer Coefficient

Experiments were conducted to determine the value of the convection heat transfer coefficient when using a rectangular winglet vortex generator (RWVG) in a common flow-down (CFD) single configuration, pair, and Reynolds number (Re) variation. Figure 5 illustrates the impact of the RWVG on increasing the convection heat transfer coefficient for both single and paired configurations. The results demonstrate that incorporating the RWVG into the test specimen significantly enhances the convection heat transfer coefficient.

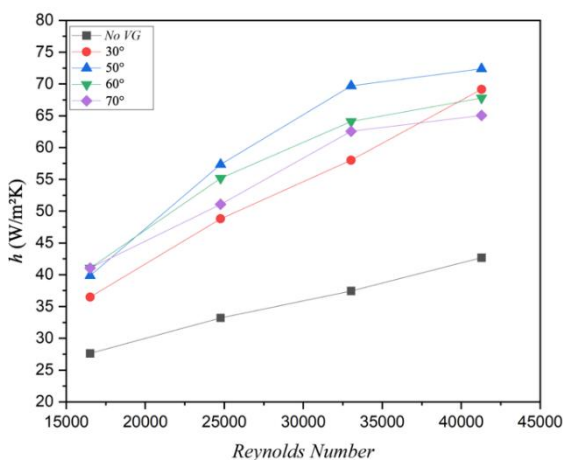
Figure 5(a) illustrates that the single rectangular winglet vortex generator (RWVG) configuration increases the convective heat transfer coefficient compared to a setup without RWVG. The incorporation of RWVG with a single configuration and varying angles of attack enhances heat transfer efficiency. This finding aligns with the modeling conducted by da Silva et al.²⁰. Current study also found that testing angles of attack (AoA) at 50° , 60° , and 70° yielded a wider range of results than da Silva et al.²⁰, which only examined the variation of AoA up to 45° . In their research, the optimal balance between heat transfer and pressure drop penalty was identified in the delta winglet at an AoA of 30° . However, the highest heat transfer results occurs at AoA of 45° ²⁰. In a study conducted by Setiawan et al.³⁷, the highest heat transfer coefficient was observed at a 50° AoA with a Reynolds number (Re) of 724, recording a value of $25.79 W/m^2K$, which represents an increase of 51.1%. Additionally, as presented in Figure 5(a), the peak convection heat transfer coefficient occurred at Re of 41,285 with an AoA of 60° , measuring $78 W/m^2K$. Conversely, the lowest convection heat transfer coefficient was found at Re of 16,514 with an AoA of 30° , at $36.82 W/m^2K$. This indicates that an increase in the heat transfer coefficient is associated with a decrease in the temperature on the surface of the

photovoltaic (PV) model. Additionally, it's noteworthy that the behavior of the RWVG varies depending on its position.

Figure 5(b) illustrates that the paired RWVG CFD configuration increases the convection heat transfer coefficient, similar to the single configuration. In this setup, the highest convection heat transfer coefficient occurs at a Reynolds number (Re) of 41,285 with an angle of attack (AoA) of 50°, reaching a value of 72.37 W/m²K. This peak heat transfer coefficient is primarily influenced by the variation in the AoA set at 50°. The enhancement in heat transfer can be attributed to a potential change in the thermal boundary layer. The temperature difference between the surface of the PV model with VG and without VG, while maintaining the same ambient temperature, results in an increased gradient in the thermal boundary layer, leading to this change. Conversely, the lowest convection heat transfer coefficient is observed at Re of 16,514 with an AoA of 30°, measuring 36.48 W/m²K. These findings indicate that the convection heat transfer coefficient increases with rising Reynolds numbers³⁸.



(a)



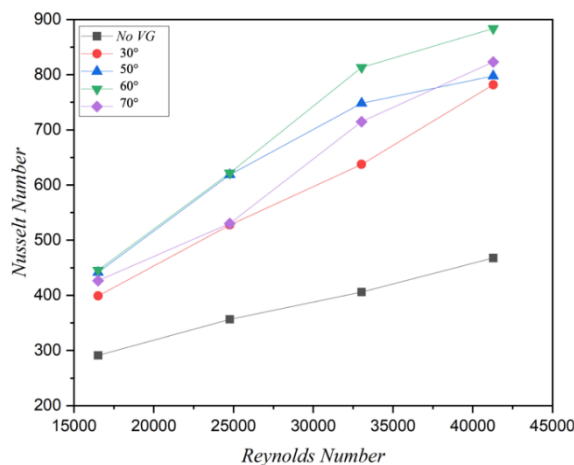
(b)

Fig. 5: Effect of RWVG CFD configuration (a) Single (b) Pair on heat transfer coefficient

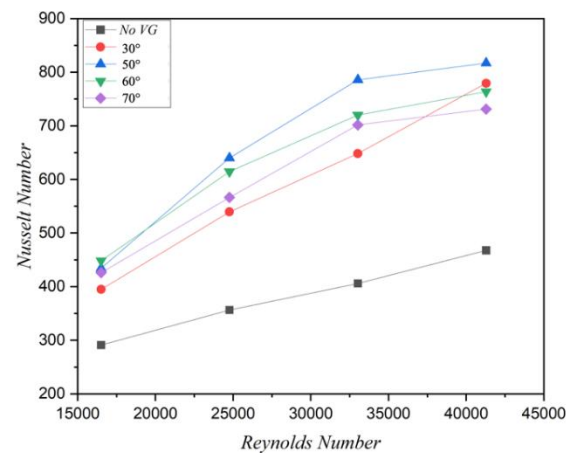
3.2. The effect of Rectangular Winglet Vortex Generator (RWVG) on Nusselt Number

The effect of using rectangular winglet vortex generator (RWVG) on heat transfer in this study is evaluated using the Nusselt Number (Nu). The study's results indicate that the use of RWVG effectively increases the Nu value. Figure 6 illustrates how RWVG contributes to this increase in Nu. The Nu is a dimensionless quantity used in heat transfer to represent the ratio of convective to conductive heat transfer³⁹. It provides insight into the effectiveness of heat transfer during fluid flow. The experimental findings reveal a consistent pattern of increasing heat transfer coefficients that aligns with the rising Nu values.

Figure 6(a) demonstrates the impact of a single RWVG configuration on variations in AoA of 30°, 50°, 60°, and 70°. The data indicates that these four attack angle variations lead to an increase in the Nu value when compared to the solar PV model without RWVG. The variation in attack angles significantly affects the Nu value at each Reynolds number (Re) condition. In the single configuration, the Nu value rises for all attack angle



(a)



(b)

Fig. 6: The effect of RWVG CFD configuration (a) Single (b) Pair on the Nusselt Number

variations. The highest Nu value, 883.57, is observed at the 60° AoA with Re of 41,285, while the lowest Nu value is 398.85 at the 30° AoA with Re of 16,514. The standard deviations were 5.8%, 5.9%, 6.1%, and 5.1%. The standard deviation increases with the Reynolds number (Re), suggesting that the angle of attack (AoA) becomes more influential as Re increases. The dominance of the highest heat transfer coefficient from the previous section contributes to the highest Nu value being reached at the 60° AoA. This finding aligns with research conducted by Leu et al.⁴⁰, which indicates that a 60° AoA yields optimal results for enhancing heat transfer, as this configuration maximizes the influence of vortices on the boundary layer. Figure 6(b) illustrates the impact of the RWVG CFD pair configuration on the AoA variations of 30°, 50°, 60°, and 70°. The experimental results indicate a consistent increase in the Nusselt number (Nu) across all tested angles. The highest Nu value of 817.23 occurs at an AoA of 50° with a Reynolds number (Re) of 41,285. In contrast, the lowest Nu is recorded at an AoA of 30°, with Re = 16,514, yielding Nu = 394.94. The graphs for the 50°, 60°, and 70° AoA variations exhibit similar characteristics. Notably, there is an increase in Nu from Re of 16,514 to 33,028, followed by stability in Nu values between Re of 33,028 and Re of 41,285. The standard deviations for each were 5.7%, 6.1%, 5.9%, and 4.7%. The CFD results show that an AoA of 50° yields the most favorable trend for increasing Nu across all Re conditions. This observation aligns with the previous data presented in Figure 5(b), which also highlights the dominance of the 50° AoA in terms of the heat transfer coefficient in this configuration. As the angle of attack (AoA) increases, the friction factor also increases due to the larger projected area⁴¹. This larger projected area leads to greater flow resistance⁴². In this study, the highest Nusselt number (Nu) was observed at an AoA of 50°, without accounting for pressure drop. Vortex generators (VGs) generate vortices and secondary flows, which significantly enhance fluid mixing. These vortical motions facilitate the efficient transport of hot fluid toward the surfaces of photovoltaic (PV) panels, thereby improving the heat transfer rate and increasing the Nusselt number (Nu).

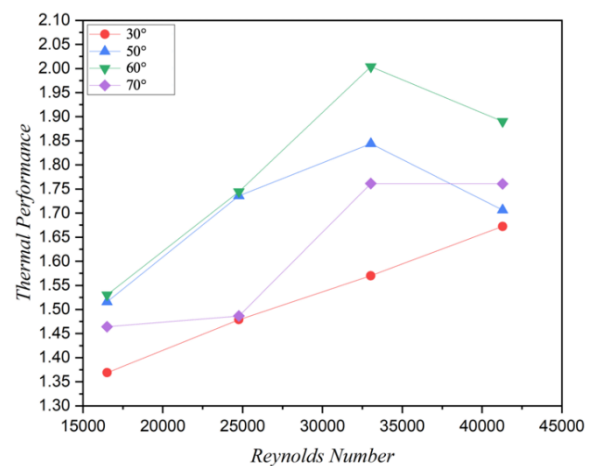
The vortex intensity increases with higher Reynolds numbers (Re); however, the secondary flow along the PV surfaces may be diminished by viscous diffusion. The secondary flows induced by the VGs modify the temperature distribution, resulting in a thinner thermal boundary layer and further enhancing the heat transfer performance⁴³. These phenomena will be effectively illustrated through temperature visualization using a thermal camera, which will be explained hereafter. At lower angles of attack, the flow predominantly generates longitudinal vortices, whereas at higher angles of attack, transverse vortices emerge, highlighting the complex interaction between flow dynamics and thermal

characteristics.

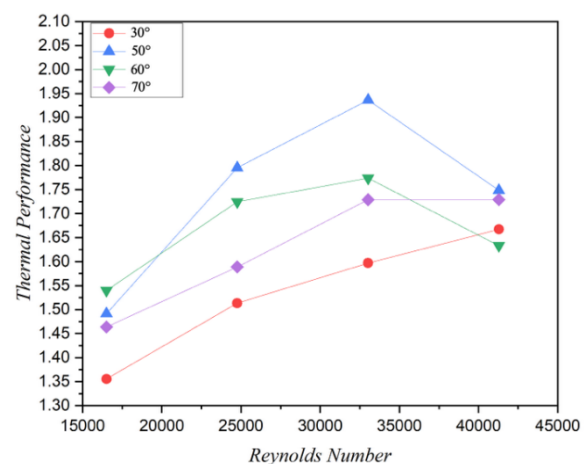
3.3. The Thermal Performance

The application of rectangular vortex generator (RWVG) enhances heat transfer, which results in an increase in the Nusselt number (Nu). Thus, thermal performance (TP) is assessed to evaluate how effectively RWVG improves heat transfer. Thermal performance refers to a system's capacity to transfer or retain heat. In this context, TP specifically denotes the efficiency of a system in transferring heat through convection.

Figure 7(a) illustrates the effect of varying the angle of attack (AoA) at 30°, 50°, 60°, and 70° on the TP value for the single RWVG configuration. In this configuration, the highest TP value, which is 2, occurs at an AoA of 60° with a corresponding Re value of 33,028. Conversely, the lowest TP value is observed at an AoA of 30°, where the Re value is 16,514 and the TP value is 1.37. Furthermore, the AoA of 60° significantly impacts performance compared to the other angles, as it achieves the best TP value across all Re conditions. This improvement is attributed to the enhanced heat transfer, as demonstrated in



(a)



(b)

Fig. 7 : The effect of configuration (common flow down) (a) Single (b) Pair on the Thermal Performance

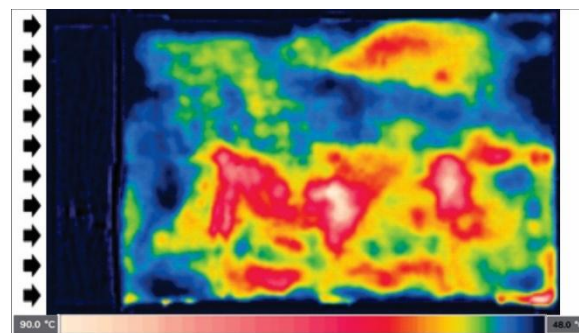
Figure 5.

Figure 6(b) illustrates the impact of varying the AoA at 30°, 50°, 60°, and 70° on the thermal performance (TP) for the RWVG CFD pair configuration. In this setup, the highest TP number is observed at an AoA of 50°, where the Reynolds number (Re) corresponds to 33,028, yielding a TP value of 1.94. In contrast, the lowest TP value of 1.36 occurs at an AoA of 30°, with a Reynolds number of 16,514. This finding aligns with the work conducted by M. Gupta et al.⁴⁴⁾, indicating that the thermal enhancement factor increases with the Reynolds number. Additionally, the characteristics of the AoA at 50°, 60°, and 70° demonstrate similar trends. As the Reynolds number increases from 16,513 to 33,028, TP values rise, peaking at this Reynolds number, before subsequently decreasing to a value of 41,285. Therefore, the three AoA reach an optimal point at a Reynolds number of 33,028.

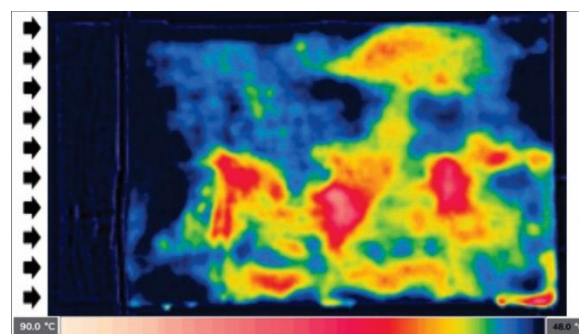
3.4. Thermal Result Visualization

A thermal camera is employed to examine the temperature distribution on the PV solar panel model. The results from the thermal camera can also be utilized to evaluate the impact of using a rectangular vortex generator (RWVG) by comparing the thermal camera outcomes with and without RWVG, considering various angles of attack. Figure 8 illustrates the surface temperature distribution of the PV model prior to the implementation of RWVG. The Figure indicates that as the Reynolds number increases, the surface temperature of the PV model decreases. The most significant temperature drop occurs at the surface inlet, while the outlet does not achieve an optimal temperature reduction. The heat generated by the heater is conducted to the surface of the PV model and is subsequently transferred by convection from the coolant flowing over the PV model. Figure 8(a) illustrates the heat distribution at a Reynolds number (Re) of 16,514. In this Figure, it can be observed that at the midpoint and outlet of the photovoltaic (PV) model surface, there is no significant decrease in temperature. At this Re value, the average temperature detected by the camera is 67.2°C, with a maximum temperature of 90.4°C. This indicates that slower fluid movement results in lower temperatures being channelled to the PV model surface, leading to heat accumulation at the back. Figure 7(b) presents the heat distribution at a Reynolds number of 24,771. In this case, a noticeable decrease in temperature occurs at the inlet point. Moreover, both the midpoint and outlet of the PV model surface show improved temperature reductions compared to the previous Re value, with the highest temperature detected at 79.7°C. Finally, Figure 8(d) depicts the heat distribution at a Reynolds number of 41,285. This condition shows the most significant temperature reduction across the inlet, middle, and outlet areas of the PV model surface without the presence of a RWVG. Although high temperatures were still observed, they were not as pronounced as in

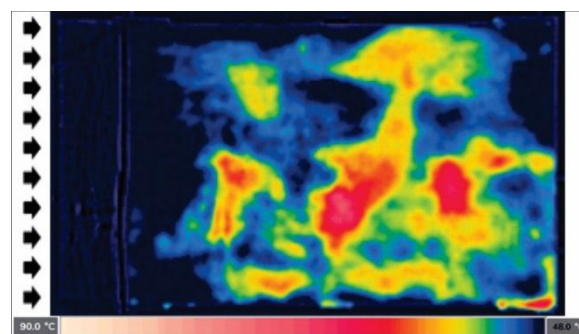
earlier conditions. Under these circumstances, the highest temperature detected was 66.7°C.



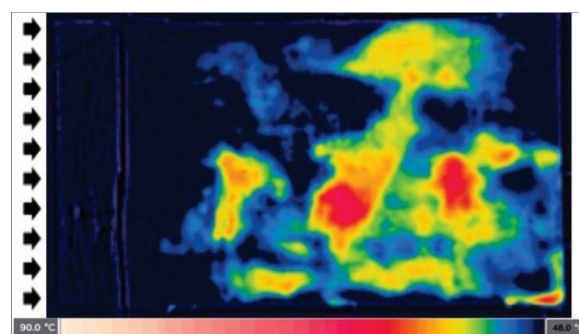
(a)



(b)



(c)



(d)

Fig. 8: Surface Temperature Distribution of Solar PV Without RWVG at Re (a) 16,514, (b) 24,771, (c) 33,028, (d) 41,285

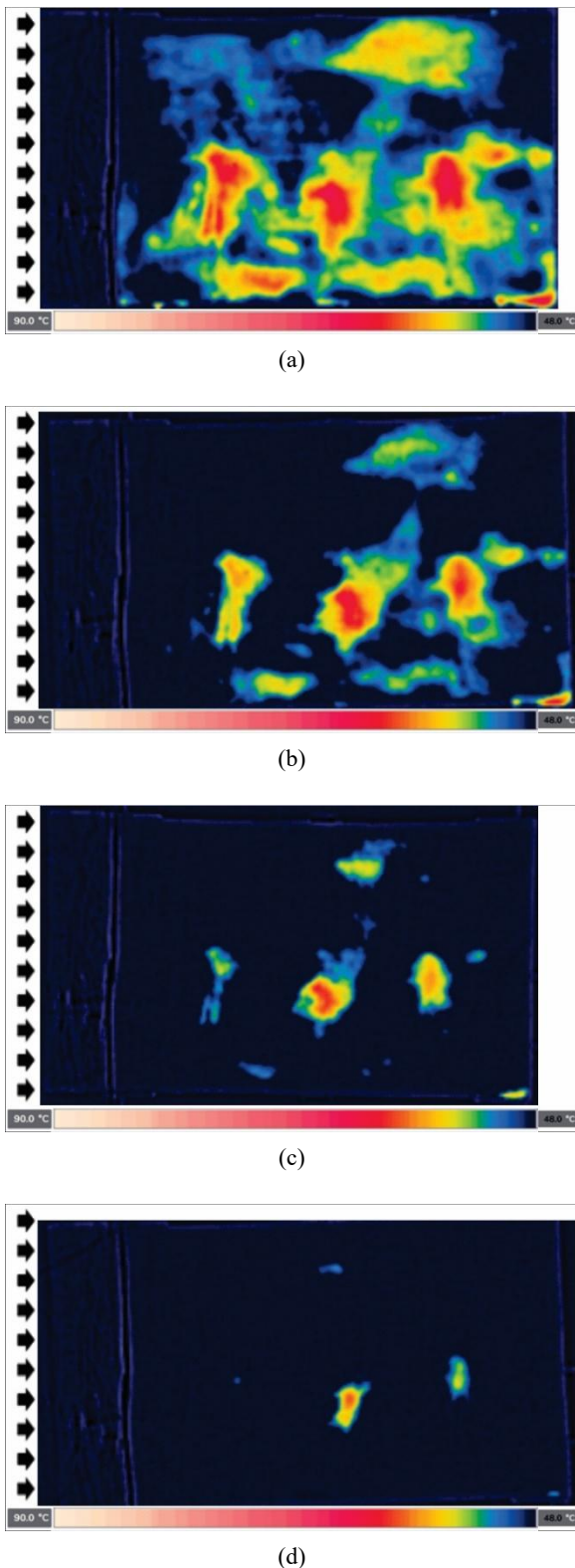


Fig. 9: Temperature distribution of PV modules with single VG under conditions AoA 60° (a) Re of 16,514, (b) Re of 24,771, (c) Re of 33,028, (d) Re of 41,285

Figure 9 illustrates the heat distribution on the surface of the PV model for a single configuration that achieves the highest TP value under various Re conditions. It is evident from the Figure that the surface of the PV model in this configuration experiences a more significant temperature

reduction compared to the model without the RWVG. This indicates that the installation of one vortex configuration effectively reduces the surface temperature. Specifically, Figure 9(a) displays the surface heat distribution at an AoA of 60° with a Reynolds number (Re) of 16,514. In this scenario, heat distribution is still noticeable but improved compared to the model without RWVG. The temperature reduction for this variation is 19.2%, with the highest recorded temperature being 66.8°C and the average surface temperature of the PV model at 50.9°C.

Figure 9 (b) illustrates the surface heat distribution of the PV model at an AoA of 60° with a Reynolds number (Re) of 24,771. Under these conditions, there is a notable reduction in temperature compared to the previous scenario, with the highest temperature recorded at 60°C. In Figure 9 (c), the surface heat distribution of the PV model is shown again at AoA of 60°, but with a higher Reynolds number of 33,028. The temperature reduction in this scenario is substantial, as indicated by the fewer red dots in the Figure. The average temperature reduction is approximately 25%, with the highest temperature reaching 55.8°C. Figure 9 (d) depicts the surface heat distribution of the PV model at the same AoA of 60°, but at a Reynolds number of 41,285. In this case, the average surface temperature reduction is 22.1%, with the highest temperature at 52.7°C. The increase in heat transfer in this condition is somewhat limited by the increase in fluid velocity and turbulence. However, the installation of RWVG enhances the mixing effect due to the eddies that are generated.

Figure 10 illustrates the heat distribution on the surface of the PV model equipped with a common flow down RWVG configuration, which achieves the highest TP value at each variation of the Reynolds number (Re). This Figure demonstrates that the surface temperature can be effectively reduced by using a RWVG in a common flow-down configuration. In Figure 10 (a), the surface heat distribution of the solar PV model is shown at an AoA of 60° with a Reynolds number (Re) of 16,514. It is evident from this Figure that there is only a slight decrease in heat compared to the condition using a single RWVG. The highest temperature detected by the thermal camera under these conditions is 65.9°C, resulting in an average temperature reduction of 19.47%.

Figure 10 (b) illustrates the surface heat distribution of the solar PV model at an angle of attack of 50° with a Reynolds number (Re) of 24,771. Under these conditions, the average surface temperature of the solar PV model decreased by 23.15%, with the thermal camera detecting a maximum temperature of 56.9°C. Figure 10 (c) presents the surface heat distribution of the solar PV model at the same AoA of 50°, but with a Reynolds number of 33,028. In this scenario, the average temperature decrease is 24.11%, and the highest temperature dropped to 51.4°C. Finally, Figure 10 (d) demonstrates the surface heat

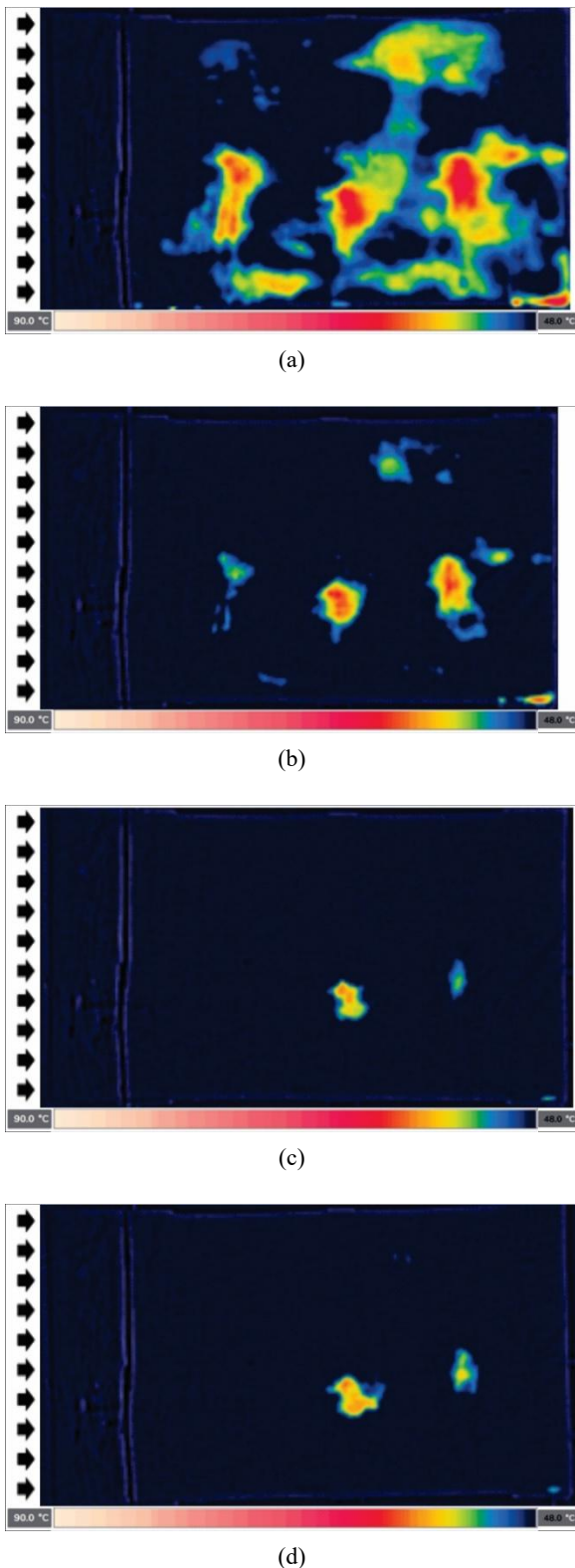


Fig. 10: Temperature distribution of PV modules with RWVG CFD configuration under conditions (a) AoA 60°, Re of 16,514, (b) AoA 50°, Re of 24,771, (c) AoA 50°, Re of 33,028, (d) AoA 50°, Re of 41,285

distribution at an AoA of 50° with a Reynolds number of 41,285. Here, the average temperature decrease is 20.3%, and the highest temperature recorded is 51.8°C. This indicates a reduction in the thermal performance (TP)

value compared to the previous condition.

4. Conclusion

The experimental study focused on a solar photovoltaic model cooling system that utilizes rectangular winglet vortex generators (RWVG) with a common-flow down configuration. Three different angles of attack (AoA), ranging from 30° to 70°, were examined under Reynolds numbers (Re) from 15,000 to 45,000. The results demonstrate that the addition of RWVG significantly enhances the heat transfer coefficient compared to the photovoltaic model without vortex generators. The most substantial increase in the single configuration occurs at an AoA of 60° with a Re of 41285, achieving an improvement of 92.45%. In the paired configuration, the greatest increase is noted at an AoA of 50° with a Re of 41,285, resulting in an enhancement of 86.25%. Furthermore, the incorporation of RWVG in the photovoltaic model greatly impacts thermal performance. The highest thermal performance value is observed in the single configuration at an AoA of 60° with a Reynolds number of 33,028. In the paired configuration, specifically in the common flow down setup at an AoA of 50° and a Reynolds number of 33,028, the thermal performance value reaches 1.94. Notably, in the paired common flow down configuration, thermal performance (TP) values for AoA of 50°, 60°, and 70° peak at a Reynolds number of 33,028.

Nomenclature

q''	heat flux (W/m ²)
V_{electric}	voltage of the heater (V)
I	electric current of the heater (A)
A_s	surface area of the solar PV model (m ²)
h	convection heat transfer coefficient (W/m ² .K)
T_s	surface temperature of the solar PV model (K)
T_{∞}	room temperature (K)
Re	reynolds number (-)
V	air velocity (m/s)
H	RWVG height (m)
ν	kinematic viscosity (m ² /s)
Nu	nusselt number (-)
k	thermal conductivity (W/m.K)
Nu_{RWVG}	nusselt number resulting from the addition of RWVG (-)
Nu_0	nusselt number without the addition of RWVG (-)

Acknowledgments

This research was financed by a PNPB grant from Universitas Sebelas Maret in Indonesia, under contract number 371/UN27.22/PT.01.03/2025. This grant is part of the Penguatan Kapasitas Grup Riset (PKGR-UNS) A scheme.

References

- 1) S. Sobri, S. Koochi-Kamali, and N.A. Rahim, "Solar photovoltaic generation forecasting methods: a review," *Energy Convers Manag*, 156 459–497 (2018). doi:10.1016/j.enconman.2017.11.019.
- 2) H. Jody, D. Mamahit, and M. Rumbayan, "Utilization of solar energy using solar panels to power a water pump [Translated from Bahasa Indonesia]," (2021).
- 3) S.M. Choi, H.G. Kwon, T. Kim, H.K. Moon, and H.H. Cho, "Active cooling of photovoltaic (pv) cell by acoustic excitation in single-dimpled internal channel," *Appl Energy*, 309 (2022). doi:10.1016/j.apenergy.2021.118466.
- 4) M.E. Kashan, A.S. Fung, J. Swift, and R. Kumar, "PV Panel Heat Transfer Rate Enhancement Using a Novel Heat Exchanger with High-Resolution Spikes and Dimples," in: *E3S Web of Conferences*, EDP Sciences, 2023. doi:10.1051/e3sconf/202339603018.
- 5) F. Al-Amri, F. Saeed, and M.A. Mujeebu, "Novel dual-function racking structure for passive cooling of solar pv panels –thermal performance analysis," *Renew Energy*, 198 100–113 (2022). doi:10.1016/j.renene.2022.08.047.
- 6) A. del Amo, A. Martínez-Gracia, A.A. Bayod-Rújula, and J. Antoñanzas, "An innovative urban energy system constituted by a photovoltaic/thermal hybrid solar installation: design, simulation and monitoring," *Appl Energy*, 186 140–151 (2017). doi:10.1016/J.APENERGY.2016.07.011.
- 7) S. Siah Chehreh Ghadikolaei, "Solar photovoltaic cells performance improvement by cooling technology: an overall review," *Int J Hydrogen Energy*, 46 (18) 10939–10972 (2021). doi:10.1016/j.ijhydene.2020.12.164.
- 8) S. Kumari, A. Bhende, A. Pandit, and S. Rayalu, "Efficiency enhancement of photovoltaic panel by heat harvesting techniques," *Energy for Sustainable Development*, 73 303-314 (2023). <https://doi.org/10.1016/j.esd.2023.02.007>.
- 9) A. Khan, P. Anand, S. Garshasbi, R. Khatun, S. Khorat, R. Hamdi, D. Niyogi, and M. Santamouris, "Rooftop photovoltaic solar panels warm up and cool down activities," *Nat Cities*, 1 780-790 (2024). <https://doi.org/10.1038/s44284-024-00137-2>.
- 10) H.M. Maghrabie, K. Elsaid, E.T. Sayed, M.A. Abdelkareem, T. Wilberforce, and A.G. Olabi, "Building-integrated photovoltaic/thermal (bipvt) systems: applications and challenges," *Sustainable Energy Technologies and Assessments*, 45 (2021). doi:10.1016/j.seta.2021.101151.
- 11) X. Zhang, A. Ding, H. Sun, and E. Rahman, "Thermodynamic limits and performance optimization of nighttime thermoradiative energy conversion systems with non-idealities," *Case Studies in Thermal Engineering*, 45 102932 (2023). doi:10.1016/J.CSITE.2023.102932.
- 12) A.G. Lupu, V.M. Homutescu, D.T. Balanescu, and A. Popescu, "A review of solar photovoltaic systems cooling technologies," in: *IOP Conf Ser Mater Sci Eng*, Institute of Physics Publishing, 2018. doi:10.1088/1757-899X/444/8/082016.
- 13) N. J. Dingo, J. Kindangen, and P. Gosal, "View of Passive Cooling Study to Improve Indoor Comfort in the Office Building of the Department of Housing and Residential Areas of South Minahasa Regency [Translated from Bahasa Indonesia]," *Jurnal Sains dan Teknologi*, 5(1), 158–169 (2023).
- 14) A. Abiyyu, "Enhancing Solar Air Heater Efficiency Using a 45° Concave-Type Vortex Generator," Bachelor's thesis, Universitas Diponegoro, Semarang, Indonesia, 2020 [in Indonesian]. doi:10.13140/RG.2.2.12054.68163.
- 15) S.K. Mohanakrishnan, Y. Yang, D.S.K. Ting, and S. Ray, "The effect of transverse spacing of a winglet pair on flat plate heat convection," *Appl Therm Eng*, 194 (2021). doi:10.1016/j.applthermaleng.2021.117094.
- 16) H.E. Ahmed, M.Z. Yusoff, M.N.A. Hawlader, M.I. Ahmed, B.H. Salman, and A.S. Kerbeet, "Turbulent heat transfer and nanofluid flow in a triangular duct with vortex generators," *Int J Heat Mass Transf*, 105 495–504 (2017). doi:10.1016/J.IJHEATMASSTRANSFER.2016.10.009.
- 17) H. Wu, D.S.K. Ting, and S. Ray, "The effect of delta winglet attack angle on the heat transfer performance of a flat surface," *Int J Heat Mass Transf*, 120 117–126 (2018). doi:10.1016/j.ijheatmasstransfer.2017.12.030.
- 18) D. Waterworth, and A. Armstrong, "Southerly winds increase the electricity generated by solar photovoltaic systems," *Solar Energy*, 202 123–135 (2020). doi:10.1016/j.solener.2020.03.085.
- 19) S. Suryo, M. Muchammad, and A. Wilarsati, "The Effect of Delta Winglet Vortex Generator Aspect Ratio on Heat Transfer from Tubes to Airflow in a Channel [Translated from Bahasa Indonesia]," *Journal Teknik Mesin*, 9 (1), 47-62 (2021).
- 20) F.A.S. da Silva, D.J. Dezan, A. V. Pantaleão, and L.O. Salviano, "Longitudinal vortex generator applied to heat transfer enhancement of a flat plate solar water heater," *Appl Therm Eng*, 158 (2019). doi:10.1016/j.applthermaleng.2019.113790.
- 21) Y.G. Lei, Y.L. He, L.T. Tian, P. Chu, and W.Q. Tao, "Hydrodynamics and heat transfer characteristics of a novel heat exchanger with delta-winglet vortex generators," *Chem Eng Sci*, 65 (5) 1551–1562 (2010). doi:10.1016/J.CES.2009.10.017.

- 22) Y. Wang, T. Zhao, Z. Cao, C. Zhai, Y. Zhou, W. Lv, T. Xu, and S. Wu, "Numerical study on the forced convection enhancement of flat-roof integrated photovoltaic by passive components," *Energy Build*, 289 113063 (2023). doi:10.1016/J.ENBUILD.2023.113063.
- 23) S. K. Mohanakrishnan, Y. Yang, D.S.-K. Ting, and S. Ray, "The effect of transverse spacing of a winglet pair on flat plate heat convection," *Applied Thermal Engineering*, 194 117094 (2021). <https://doi.org/10.1016/j.applthermaleng.2021.117094>.
- 24) D.J. Dezan, A.D. Rocha, L.O. Salviano, and W.G. Ferreira, "Thermo-hydraulic optimization of a solar air heater duct with non-periodic rows of rectangular winglet pairs," *Solar Energy*, 207 1172–1190 (2020). doi:10.1016/j.solener.2020.06.112.
- 25) A.J. Modi, and M.K. Rathod, "Experimental investigation of heat transfer enhancement and pressure drop of fin-and-circular tube heat exchangers with modified rectangular winglet vortex generator," *Int J Heat Mass Transf*, 189 (2022). doi:10.1016/j.ijheatmasstransfer.2022.122742.
- 26) O. Heriyani, M. Djaeni, Syaiful, and A.K. Putri, "Perforated concave rectangular winglet pair vortex generators enhance the heat transfer of air flowing through heated tubes inside a channel," *Results in Engineering*, 16 (2022). doi:10.1016/j.rineng.2022.100705.
- 27) S.K. Sarangi, and D.P. Mishra, "A comprehensive review on vortex generator supported heat transfer augmentation techniques in heat exchangers," *J Therm Anal Calorim*, 149 (15) 7839–7867 (2024). doi:10.1007/s10973-024-13369-0.
- 28) M. Sheikholeslami, and F.A.M. Abd Ali, "Experimental evaluation of vortex generators for enhancing solar photovoltaic panel performance with parabolic reflectors," *Sol. Energy Mater. Sol. Cells.*, 282 113411 (2025). <https://doi.org/10.1016/j.solmat.2025.113411>.
- 29) B. Souayah, S. Bhattacharyya, J. Saad, Z. Alherz, K. Dey, and A. Advait, "Enhanced thermal management of solar PV panels using magnetic nanofluid with external magnetic swirl generator," *Case Studies in Thermal Engineering*, 70 106087 (2025), <https://doi.org/10.1016/j.csite.2025.106087>.
- 30) S. M. Choi, H. G. Kwon, H. M. Bae, H. K. Moon, and H. H. Cho, "Effects of staggered dimple array under different flow conditions for enhancing cooling performance of solar systems," *Applied Energy*, 342 121120 (2023). doi:10.1016/j.apenergy.2023.121120.
- 31) S. Ali, C. Habchi, H. Zaytoun, M. Khaled, and T. Dbouk, "Surrogate-based optimization of the attack and inclination angles of a delta winglet pair vortex generator in turbulent channel flow," *International Journal of Thermofluids*, 20 100473 (2023). doi:10.1016/j.ijft.2023.100473.
- 32) G. S. Sabet, A. Sari, A. Fakhari, N. Afsarimanesh, D. Organ, and S. M. Hoseini, "An Experimental and Numerical Thermal Flow Analysis in a Solar Air Collector with Different Delta Wing Height Ratios," *Frontiers in Heat and Mass Transfer*, 22 (2) 491–509 (2024) doi: 10.32604/fhmt.2024.048290.
- 33) Z. Zhou et al., "Passive PV module cooling under free convection through vortex generators," *Renewable Energy*, 190 319–329 (2022) doi: 10.1016/j.renene.2022.03.133.
- 34) Z. Zhou, A. Gentle, M. Mohsenzadeh, Y. Jiang, M. Keevers, and M. Green, "Long-term outdoor testing of vortex generators for passive PV module cooling," *Solar Energy*, 275 112610 (2024). <https://doi.org/10.1016/j.solener.2024.112610>.
- 35) M. Sheikholeslami, and F.A.M. Abd Ali, "Experimental evaluation of vortex generators for enhancing solar photovoltaic panel performance with parabolic reflectors," *Solar Energy Materials and Solar Cells*, 282 113411 (2025). <https://doi.org/10.1016/j.solmat.2025.113411>.
- 36) G. Marausna, E. E. Prasetyo, and F. Setiawan, "The use of wavy vortex generates in the cooling system to reduce the photovoltaic temperature rises," *International Journal of Power Electronics and Drive Systems*, 14 (2) 1210 – 1217 (2023). DOI: 10.11591/ijpeds.v14.i2.pp1210-1217.
- 37) R. C. Setiawan, I. Yaningsih, D. D. D. P., Tjahjana, A. R. Prabowo, K. Enoji, K. Thu, and T. Miyazaki, "Thermal Performance Evaluation of Solar PV Cooling Model with Rectangular Winglet Pair Vortex Generator Application," *Evergreen*, 12 (1) 71–80 (2025). doi: 10.5109/7342439.
- 38) M. Awais, and A.A. Bhuiyan, "Enhancement of thermal and hydraulic performance of compact finned-tube heat exchanger using vortex generators (vgs): a parametric study," *International Journal of Thermal Sciences*, 140 154–166 (2019). doi:10.1016/J.IJTHERMALSCI.2019.02.041.
- 39) A.A. Kornhauser, and J.L. Smith, "Application of a Complex Nusselt Number to Heat Transfer During Compression and Expansion," 1994. <http://heattransfer.asmedigitalcollection.asme.org/>.
- 40) J.S. Leu, Y.H. Wu, and J.Y. Jang, "Heat transfer and fluid flow analysis in plate-fin and tube heat exchangers with a pair of block shape vortex generators," *Int J Heat Mass Transf*, 47 (19–20) 4327–4338 (2004). doi:10.1016/j.ijheatmasstransfer.2004.04.031.
- 41) . Li Zhang, X. Yan, Y. Zhang, Y. Feng, Y. Li, H. Meng, J. Zhang, and J. Wu, "Heat transfer enhancement by streamlined winglet pair vortex

generators for helical channel with rectangular cross section,” *Chemical Engineering and Processing - Process Intensification*. 147 107788 (2020) <https://doi.org/10.1016/j.cep.2019.107788>.

- 42) M. Fiebig, P. Kallweit, and N. Mitra, “Heat transfer enhancement and drag by longitudinal VGs in channel flow,” *Exp. Therm. Fluid Sci.* 4 103–114 (1991). [https://doi.org/10.1016/0894-1777\(91\)90024-L](https://doi.org/10.1016/0894-1777(91)90024-L).
- 43) A. Abdollahi and M. Shams, Optimization of shape and angle of attack of winglet vortex generator in a rectangular channel for heat transfer enhancement,” *Applied Thermal Engineering* 81 376-387 (2015). <https://doi.org/10.1016/j.applthermaleng.2015.01.044>.
- 44) M. Gupta, K.S. Kasana, and R. Vasudevan, “Heat transfer augmentation in a plate-fin heat exchanger using a rectangular winglet,” *Heat Transfer - Asian Research*, 39 (8) 590–610 (2010). [doi:10.1002/htj.20318](https://doi.org/10.1002/htj.20318).